

# Tensor Entropy for Uniform Hypergraphs

Can Chen, Indika Rajapakse

**Abstract**—In this paper, we develop the notion of entropy for uniform hypergraphs via tensor theory. We employ the probability distribution of the generalized singular values, calculated from the higher-order singular value decomposition of the Laplacian tensors, to fit into the Shannon entropy formula. We show that this tensor entropy is an extension of von Neumann entropy for graphs. In addition, we establish results on the lower and upper bounds of the entropy and demonstrate that it is a measure of regularity for uniform hypergraphs in simulated and experimental data. We exploit the tensor train decomposition in computing the proposed tensor entropy efficiently. Finally, we introduce the notion of robustness for uniform hypergraphs.

**Index Terms**—uniform hypergraphs, entropy, tensor decompositions, pattern recognition, random hypergraphs.

## 1 INTRODUCTION

MANY real world complex systems can be decomposed and analyzed using networks. There are two classical types of complex networks, scale-free networks and small world networks, which have provided insights in social sciences, cell biology, neuroscience and computer science [1], [2], [3], [4]. Recent advancements in genomics technology, such as genome-wide chromosome conformation capture (Hi-C), have inspired us to consider the human genome as a dynamic graph [5], [6]. Studying such dynamic graphs often requires identifying the changes in network properties, such as degree distribution, path lengths and clustering coefficients [7], [8], [9].

Numerous techniques have been developed for anomaly detection based on evaluating similarities between graphs [10], [11]. A classic approach for detecting anomalous timestamps during the evolution of dynamic graphs is comparing two consecutive graphs using distance or similarity functions. A comprehensive survey on similarity measures can be found in [12]. Two popular measures, Hamming distance [13] and Jaccard distance [14], are often problem-specific and sensitive to small perturbations or scaling, thus providing limited understanding of variations between graphs [15]. Model-agnostic approaches, such as eigenvalue based/spectral measures, are more flexible in their representations and interpretations. Therefore, these approaches can more appropriately quantify the global structural complexity of graphs [16], [17], [18].

The von Neumann entropy of a graph, first introduced by Braunstein et al. [19], is a spectral measure used in structural pattern recognition. The intuition behind the measure is linking the graph Laplacian to density matrices from quantum mechanics, and measuring the complexity of the graphs via the von Neumann entropy of the corresponding

density matrices [20]. Additionally, the measure can be viewed as the information theoretic Shannon entropy, i.e.,

$$S = - \sum_j \eta_j \ln \eta_j, \quad (1)$$

where,  $\eta_j$  are the normalized eigenvalues of the Laplacian matrix of a graph such that  $\sum_j \eta_j = 1$ . Passerini and Severini observed that the von Neumann entropy of a graph tends to grow with the number of connected components, the reduction of long paths and the increase of nontrivial symmetricity, and suggested that it can be viewed as a measure of regularity [21]. They also showed that the entropy (1) is upper bounded by  $\ln(n-1)$  where  $n$  is the number of vertices of a graph.

However, most data representations are multidimensional, and using graph models to describe them may lose information [22]. A hypergraph is a generalization of a graph in which a hyperedge can join any number of vertices [23], see Figure 1. Thus, hypergraphs can represent multidimensional relationship unambiguously [22]. Examples of hypergraphs include co-authorship networks, film actor/actress networks and protein-protein interaction networks [24]. The authors in [22] also mention that hypergraphs require less storage space than graphs which may accelerate computation. Moreover, a hypergraph can be represented by a tensor if its hyperedges contain the same number of vertices (referred to as a uniform hypergraph). Tensors are multidimensional arrays generalized from vectors and matrices, preserving multidimensional patterns and capturing higher-order interactions and couplings within multiway data [25]. Tensor decompositions such as CANDECOMP/PARAFAC decomposition (CPD), higher-order singular value decomposition (HOSVD) and tensor train decomposition (TTD) can not only facilitate computation, but they also contain contextual interpretations regarding the target data tensors [26], [27], [28], [29].

Hypergraph entropy has been recently explored by Hu et al. [30], Wang et al. [31] and Bloch et al. [32]. In particular, the authors in [30] employ the probability distribution of the vertex degrees to fit into the Shannon entropy formula and establish its lower and upper bounds for special hypergraphs. Furthermore, the authors in [31] compute the

- C. Chen is with Department of Mathematics and Department of Electrical Engineering and Computer Science, University of Michigan, Ann Arbor, MI, 48109.  
E-mail: [canc@umich.edu](mailto:canc@umich.edu)
- I. Rajapakse is with the Department of Computational Medicine & Bioinformatics, Medical School and Department of Mathematics, University of Michigan, Ann Arbor, MI, 48109.  
E-mail: [indikar@umich.edu](mailto:indikar@umich.edu)

Manuscript received March 24, 2022.

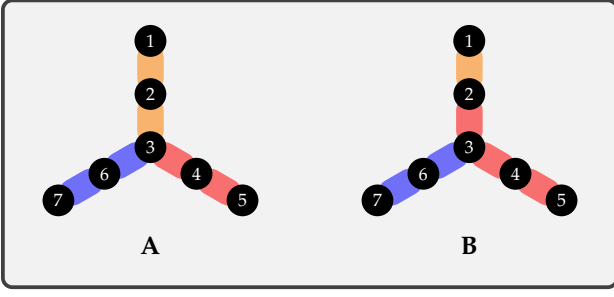


Figure 1. **Hypergraphs.** (A) A 3-uniform hypergraph with hyperedges  $e_1 = \{1, 2, 3\}$ ,  $e_2 = \{3, 4, 5\}$  and  $e_3 = \{3, 6, 7\}$ . (B) A non-uniform hypergraph with hyperedges  $e_1 = \{1, 2\}$ ,  $e_2 = \{2, 3, 4, 5\}$  and  $e_3 = \{3, 6, 7\}$ .

hypergraph entropy based on the vertex weighting scores defined by Sampson distance under some kernel functions. However, such entropies only contain partial information regarding the underlying structural properties of hypergraphs. Based on the previous works [20], [21], [33], here we develop a novel method called tensor-based hypergraph entropy, which can decipher the topological attributes of uniform hypergraphs. The key contributions of this paper are as follows:

- We propose a new notion of entropy for uniform hypergraphs based on the HOSVD of the corresponding Laplacian tensors. We establish results on the lower and upper bounds of the proposed tensor entropy, and provide a formula for computing the entropy of complete uniform hypergraphs.
- We adapt a fast and memory efficient TTD-based computational framework in computing the proposed tensor entropy for uniform hypergraphs.
- We create two simulated datasets, including a hyperedge growth model and a Watts-Strogatz model for uniform hypergraphs. We demonstrate that the proposed tensor entropy is a measure of regularity relying on the vertex degrees, path lengths, clustering coefficients and nontrivial symmetry for uniform hypergraphs. Three real world examples, a primary school contact dataset, a mouse neuron endomicroscopy dataset and a cellular reprogramming dataset, are presented as applications. The final example aims to exhibit the efficacy of the TTD-based computational framework in computing the proposed tensor entropy.
- We perform preliminary explorations of tensor eigenvalues in the entropy computation and the notion of robustness for uniform hypergraphs.

The paper is organized into five sections. We start with the basics of tensor algebra including tensor products, tensor unfolding, higher-order singular value decomposition and tensor train decomposition in section 2.1. We then propose a new form of entropy for uniform hypergraphs in section 2.2 based on the tensor algebra. We also establish results on the lower and upper bounds of the tensor entropy, and provide a direct formula for complete uniform hypergraphs. In section 2.3, we exploit the tensor train decomposition to accelerate the tensor entropy computation. Six numerical

examples are presented in section 3. Finally, we discuss some directions for future research in section 4 and conclude in section 5.

## 2 METHOD

### 2.1 Tensor preliminaries

We take most of the concepts and notations for tensor algebra from the comprehensive works of Kolda et al. [34], [35]. A *tensor* is a multidimensional array. The *order* of a tensor is the number of its dimensions. A  $k$ -th order tensor usually is denoted by  $\mathbf{X} \in \mathbb{R}^{n_1 \times n_2 \times \dots \times n_k}$ . It is therefore reasonable to consider scalars  $x \in \mathbb{R}$  as zero-order tensors, vectors  $\mathbf{v} \in \mathbb{R}^n$  as first-order tensors, and matrices  $\mathbf{A} \in \mathbb{R}^{m \times n}$  as second-order tensors. For a third-order tensor, fibers are commonly named as column ( $X_{:j_2 j_3}$ ), row ( $X_{j_1 :j_3}$ ) and tube ( $X_{j_1 j_2 :}$ ), while slices are named as horizontal ( $X_{j_1 :}$ ), lateral ( $X_{:j_2 :}$ ) and frontal ( $X_{::j_3}$ ), see Figure 2. A tensor is called *cubical* if every mode is the same size, i.e.,  $\mathbf{X} \in \mathbb{R}^{n \times n \times \dots \times n}$ . A cubical tensor  $\mathbf{X}$  is called *supersymmetric* if  $X_{j_1 j_2 \dots j_k}$  is invariant under any permutation of the indices, and is called *diagonal* if  $X_{j_1 j_2 \dots j_k} = 0$  except  $j_1 = j_2 = \dots = j_k$ .

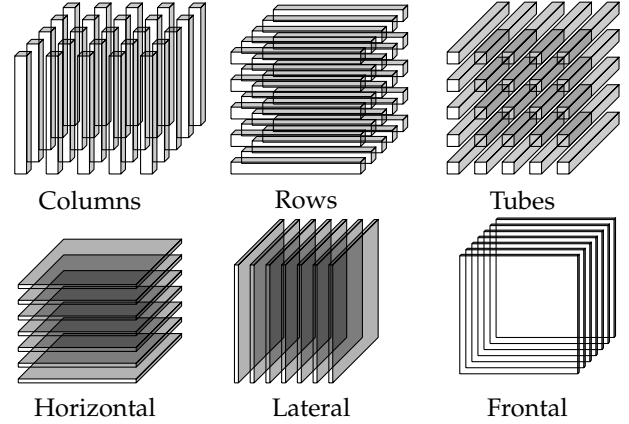


Figure 2. **Fibers and slices of a third-order tensor.** The figure is adapted from [34].

There are several notions of tensor products. The *inner product* of two tensors  $\mathbf{X}, \mathbf{Y} \in \mathbb{R}^{n_1 \times n_2 \times \dots \times n_k}$  is defined as

$$\langle \mathbf{X}, \mathbf{Y} \rangle = \sum_{j_1=1}^{n_1} \dots \sum_{j_k=1}^{n_k} X_{j_1 j_2 \dots j_k} Y_{j_1 j_2 \dots j_k}, \quad (2)$$

leading to the *tensor Frobenius norm*  $\|\mathbf{X}\|^2 = \langle \mathbf{X}, \mathbf{X} \rangle$ . We say two tensors  $\mathbf{X}$  and  $\mathbf{Y}$  are orthogonal if the inner product  $\langle \mathbf{X}, \mathbf{Y} \rangle = 0$ . The *matrix tensor multiplication*  $\mathbf{X} \times_p \mathbf{A}$  along mode  $p$  for a matrix  $\mathbf{A} \in \mathbb{R}^{m \times n_p}$  is defined by

$$(\mathbf{X} \times_p \mathbf{A})_{j_1 j_2 \dots j_{p-1} j_{p+1} \dots j_k} = \sum_{j_p=1}^{n_p} X_{j_1 j_2 \dots j_p \dots j_k} A_{j_p}. \quad (3)$$

This product can be generalized to what is known as the *Tucker product*, for  $\mathbf{A}_p \in \mathbb{R}^{m_p \times n_p}$ ,

$$\begin{aligned} & \mathbf{X} \times_1 \mathbf{A}_1 \times_2 \mathbf{A}_2 \times_3 \dots \times_k \mathbf{A}_k \\ &= \mathbf{X} \times \{\mathbf{A}_1, \mathbf{A}_2, \dots, \mathbf{A}_k\} \in \mathbb{R}^{m_1 \times m_2 \times \dots \times m_k}. \end{aligned} \quad (4)$$

Tensor unfolding is considered as a critical operation in tensor computations [35], [36], [37]. The  $p$ -mode unfolding of a tensor  $\mathbf{X} \in \mathbb{R}^{n_1 \times n_2 \times \dots \times n_k}$ , denoted by  $\mathbf{X}_p$ , is defined by

$$\mathbf{X}_{j_1 j_2 \dots j_k} = (\mathbf{X}_p)_{j_p j} \text{ for } j = 1 + \sum_{\substack{m=1 \\ m \neq p}}^k (j_m - 1) \prod_{\substack{i=1 \\ i \neq p}}^{m-1} n_i. \quad (5)$$

The ranks of the  $p$ -mode unfoldings are called *multilinear ranks* of  $\mathbf{X}$ , which are related to the so-called Higher-Order Singular Value Decomposition (HOSVD), a multilinear generalization of the matrix Singular Value Decomposition (SVD) [33], [38].

**Theorem 1** (HOSVD [33]). *A tensor  $\mathbf{X} \in \mathbb{R}^{n_1 \times n_2 \times \dots \times n_k}$  can be written as*

$$\mathbf{X} = \mathbf{S} \times_1 \mathbf{U}_1 \times_2 \dots \times_k \mathbf{U}_k, \quad (6)$$

where,  $\mathbf{U}_p \in \mathbb{R}^{n_p \times n_p}$  are unitary matrices, and  $\mathbf{S} \in \mathbb{R}^{n_1 \times n_2 \times \dots \times n_k}$  is a tensor of which the subtensors  $\mathcal{S}_{j_p=\alpha}$ , obtained by fixing the  $p$ -th index to  $\alpha$ , have the properties of

- 1) *all-orthogonality: two subtensors  $\mathcal{S}_{j_p=\alpha}$  and  $\mathcal{S}_{j_p=\beta}$  are orthogonal for all possible values of  $p, \alpha$  and  $\beta$  subject to  $\alpha \neq \beta$ ;*
- 2) *ordering:  $\|\mathcal{S}_{j_p=1}\| \geq \dots \geq \|\mathcal{S}_{j_p=n_p}\| \geq 0$  for all possible values of  $p$ .*

The Frobenius norms  $\|\mathcal{S}_{j_p=j}\|$ , denoted by  $\gamma_j^{(p)}$ , are the  $p$ -mode singular values of  $\mathbf{X}$ .

De Lathauwer et al. [33] showed that the  $p$ -mode singular values from the HOSVD of  $\mathbf{X}$  are the singular values of the  $p$ -mode unfoldings  $\mathbf{X}_p$ . In section 2.2, we will use the notion of  $p$ -mode singular values as the main tool to define the tensor entropy for uniform hypergraphs.

The Tensor Train Decomposition (TTD) of an  $k$ -th order tensor  $\mathbf{X} \in \mathbb{R}^{n_1 \times n_2 \times \dots \times n_k}$  is given by

$$\mathbf{X} = \sum_{r_k=1}^{R_k} \dots \sum_{r_0=1}^{R_0} \mathbf{X}_{r_0:r_1}^{(1)} \circ \mathbf{X}_{r_1:r_2}^{(2)} \circ \dots \circ \mathbf{X}_{r_{k-1}:r_k}^{(k)}, \quad (7)$$

where,  $\circ$  is the outer product,  $\{R_0, R_1, \dots, R_k\}$  is the set of TT-ranks with  $R_0 = R_k = 1$ , and  $\mathbf{X}^{(p)} \in \mathbb{R}^{R_{p-1} \times n_p \times R_p}$  are called the core tensors of the TTD. There exist optimal TT-ranks for the TTD such that

$$R_p = \text{reshape}(\mathbf{X}, \prod_{j=1}^p n_j, \prod_{j=p+1}^k n_j),$$

for  $p = 1, 2, \dots, k-1$  [39]. A core tensor  $\mathbf{X}^{(p)}$  is called *left-orthonormal* if  $(\bar{\mathbf{X}}^{(p)})^\top \bar{\mathbf{X}}^{(p)} = \mathbf{I} \in \mathbb{R}^{R_p \times R_p}$ , and is called *right-orthonormal* if  $\underline{\mathbf{X}}^{(p)} (\underline{\mathbf{X}}^{(p)})^\top = \mathbf{I} \in \mathbb{R}^{R_{p-1} \times R_{p-1}}$  where

$$\bar{\mathbf{X}}^{(p)} = \text{reshape}(\mathbf{X}^{(p)}, R_{p-1} n_p, R_p),$$

$$\underline{\mathbf{X}}^{(p)} = \text{reshape}(\mathbf{X}^{(p)}, R_{p-1}, n_p R_p),$$

are the left- and right-unfoldings of the core tensor, respectively. Here  $\mathbf{I}$  denotes the identity matrix, and `reshape` refers to the reshape operation in MATLAB. Basic tensor algebra, such as addition, tensor products and norms, can be done in the TT-format without requiring to recover back to the full tensor representation [39].

## 2.2 Tensor entropy

Mathematically, a *hypergraph*  $\mathbf{G} = \{\mathbf{V}, \mathbf{E}\}$  where  $\mathbf{V} = \{1, 2, \dots, n\}$  is the vertex set and  $\mathbf{E} = \{e_1, e_2, \dots, e_m\}$  is the *hyperedge* set with  $e_p \subseteq \mathbf{V}$  for  $p = 1, 2, \dots, m$  [40], [41], [42], [43], [44], [45], [46]. If all hyperedges contain the same number of nodes, i.e.,  $|e_p| = k$ ,  $\mathbf{G}$  is called a *k-uniform hypergraph*, see Figure 1. Two vertices are called *adjacent* if they are in the same hyperedge. A hypergraph is called *connected* if given two vertices, there is a path connecting them through hyperedges. Given any  $k$  vertices, if they are contained in one hyperedge, then  $\mathbf{G}$  is called *complete*. A  $k$ -uniform hypergraph can be represented by a  $k$ -th order  $n$ -dimensional supersymmetric adjacency tensor  $\mathbf{A} \in \mathbb{R}^{n \times n \times \dots \times n}$  with

$$\mathbf{A}_{j_1 j_2 \dots j_k} = \begin{cases} \frac{1}{(k-1)!} & \text{if } (j_1, j_2, \dots, j_k) \in \mathbf{E} \\ 0, & \text{otherwise} \end{cases}. \quad (8)$$

The degree tensor  $\mathbf{D}$  of a hypergraph  $\mathbf{G}$ , associated with  $\mathbf{A}$ , is also a  $k$ -th order  $n$ -dimensional diagonal tensor with  $\mathbf{D}_{j j \dots j}$  equal to the number of hyperedges that consist of  $v_j$  for  $j = 1, 2, \dots, n$ . If  $\mathbf{D}_{j j \dots j} = d$  for all  $j$ , then  $\mathbf{G}$  is called *d-regular*. Similar to Laplacian matrices, the Laplacian tensor  $\mathbf{L} \in \mathbb{R}^{n \times n \times \dots \times n}$  of  $\mathbf{G}$ , which is supersymmetric, thus is defined as

$$\mathbf{L} = \mathbf{D} - \mathbf{A}. \quad (9)$$

**Definition 1.** *Let  $\mathbf{G}$  be a  $k$ -uniform hypergraph with  $n$  vertices. The tensor entropy of  $\mathbf{G}$  is defined by*

$$\mathbf{S} = - \sum_{j=1}^n \hat{\gamma}_j \ln \hat{\gamma}_j, \quad (10)$$

where,  $\hat{\gamma}_j$  are the normalized  $k$ -mode singular values of  $\mathbf{L}$  such that  $\sum_{j=1}^n \hat{\gamma}_j = 1$ .

The convention  $0 \ln 0 = 0$  is used if  $\hat{\gamma}_j = 0$ . The  $k$ -mode singular values of  $\mathbf{L}$  can be computed from the matrix SVD of the  $k$ -mode unfolding  $\mathbf{L}_k$ , which results in a  $\mathcal{O}(n^{k+1})$  time complexity and a  $\mathcal{O}(n^k)$  space complexity, see Algorithm 1. Since  $\mathbf{L}$  is supersymmetric, any mode unfolding of  $\mathbf{L}$  would yield the same unfolding matrix with the same singular values. Moreover, the tensor entropy (10) can be viewed as a variation of von Neumann entropy defined for graphs, in which we regard  $c \mathbf{L}_k \mathbf{L}_k^\top$  as the density matrix for some normalization constant  $c$  [20], [21], [47]. In particular, when  $k = 2$ , the tensor entropy is reduced to the classical von Neumann entropy for graphs. Like the eigenvalues of Laplacian matrices, the  $k$ -mode singular values play a significant role in identifying the structural patterns for uniform hypergraphs.

**Lemma 1.** *Suppose that  $\mathbf{G}$  is a  $k$ -uniform hypergraph with  $k \geq 3$ . If  $\mathbf{L}$  has a  $k$ -mode singular value zero, with multiplicity  $p$ , then  $\mathbf{G}$  contains  $p$  number of non-connected vertices.*

*Proof.* The result follows immediately from the definitions of Laplacian tensor and  $k$ -mode unfolding of  $\mathbf{L}$ .  $\square$

**Proposition 1.** *Suppose that  $\mathbf{G}$  is a  $k$ -uniform hypergraph with  $k \geq 3$  and nonempty hyperedge set  $\mathbf{E}$ . Then the minimum tensor entropy of  $\mathbf{G}$  is given by*

$$\mathbf{S}_{\min} = \ln k. \quad (11)$$

**Algorithm 1:** Computing tensor entropy from SVD

- 1: Given a  $k$ -uniform hypergraph  $\mathbf{G}$  with  $n$  vertices
- 2: Construct the adjacency tensor  $\mathbf{A} \in \mathbb{R}^{n \times n \times \dots \times n}$  from  $\mathbf{G}$  and compute the Laplacian tensor  $\mathbf{L} = \mathbf{D} - \mathbf{A}$  where  $\mathbf{D}$  is the degree tensor
- 3: Find the  $k$ -mode unfolding of  $\mathbf{L}$ , i.e.,  $\mathbf{L}_k = \text{reshape}(\mathbf{L}, n, n^{k-1})$
- 4: Compute the economy-size matrix SVD of  $\mathbf{L}_k$ , i.e.,  $\mathbf{L}_k = \mathbf{USV}^\top$  and let  $\{\gamma_j\}_{j=1}^n = \text{diag}(\mathbf{S})$
- 5: Set  $\hat{\gamma}_j = \frac{\gamma_j}{\sum_{i=1}^n \gamma_i}$  and compute  $\mathbf{S} = -\sum_{j=1}^n \hat{\gamma}_j \ln \hat{\gamma}_j$
- 6: **return** The tensor entropy  $\mathbf{S}$  of  $\mathbf{G}$ .

*Proof.* Since  $\mathbf{G}$  is a  $k$ -uniform hypergraph on  $n$  vertices, the maximum multiplicity of the zero normalized  $k$ -mode singular value of  $\mathbf{L}$  is  $n - k$  according to Lemma 1. In addition, the other normalized  $k$ -mode singular values of are necessarily  $\frac{1}{k}$ . Hence, it is straightforward to show that  $S_{\min} = \ln k$ .  $\square$

**Proposition 2.** Suppose that  $\mathbf{G}$  is a  $k$ -uniform hypergraph with  $n$  vertices for  $k \geq 3$ . Then the maximum tensor entropy of  $\mathbf{G}$  occurs when it is a 1-regular uniform hypergraph, and is given by

$$S_{\max} = \ln n. \quad (12)$$

*Proof.* Since  $\mathbf{G}$  is a  $k$ -uniform hypergraph on  $n$  vertices, the maximum tensor entropy occurs when the multiplicity of a normalized  $k$ -mode singular value of  $\mathbf{L}$  is  $n$ . Based on the definitions of Laplacian tensor and  $k$ -mode unfolding, for a 1-regular uniform hypergraph, the number of nonzero elements in  $\mathbf{L}_k$  are fixed for  $j$ -th row with one entry

$$(\mathbf{L}_k)_{j[1+\sum_{m=1}^{k-1}(j-1)n^{m-1}]} = 1$$

and  $(k-1)!$  entries  $-\frac{1}{2}$  for  $j = 1, 2, \dots, n$ . Moreover, since all the hyperedges contain distinct vertices, the column indices of the nonzero entries are unique for  $\mathbf{L}_k$ . Thus,  $\mathbf{L}_k \mathbf{L}_k^\top$  is a diagonal matrix with equal diagonal elements, and the result follows immediately.  $\square$

**Proposition 3.** Suppose that  $\mathbf{G}$  is a  $k$ -uniform hypergraph with  $n$  vertices for  $k \geq 3$ . If  $\log_k n$  is an integer, then the maximum tensor entropy of  $\mathbf{G}$  can be achieved when it is a  $d$ -regular uniform hypergraph for  $1 \leq d \leq \log_k n$ .

*Proof.* Suppose that  $\log_k n$  is an integer. Any two hyperedges of a  $d$ -regular uniform hypergraph contain at least  $k-1$  distinct vertices for  $1 \leq d \leq \log_k n$ . Similar to Proposition 2, it can be shown that  $\mathbf{L}_k \mathbf{L}_k^\top$  is a diagonal matrix with equal diagonal elements. Therefore, the result follows immediately.  $\square$

**Proposition 4.** Suppose that  $\mathbf{G}$  is a complete  $k$ -uniform hypergraph with  $n$  vertices for  $k \geq 3$ . Then the tensor entropy of  $\mathbf{G}$  is given by

$$S_c = \frac{(1-n)\alpha}{(n-1)\alpha + \beta} \ln \frac{\alpha}{(n-1)\alpha + \beta} - \frac{\beta}{(n-1)\alpha + \beta} \ln \frac{\beta}{(n-1)\alpha + \beta} \quad (13)$$

where,

$$\alpha = \left( \frac{\Gamma(n)(\Gamma(n-k+1) + \Gamma(n))}{\Gamma(k)^2 \Gamma(n-k+1)^2} - \frac{\Gamma(n-1)}{\Gamma(k)^2 \Gamma(n-k)} \right)^{\frac{1}{2}}, \quad (14)$$

$$\beta = \left( \frac{\Gamma(n)(\Gamma(n-k+1) + \Gamma(n))}{\Gamma(k)^2 \Gamma(n-k+1)^2} + \frac{(n-1)\Gamma(n-1)}{\Gamma(k)^2 \Gamma(n-k)} \right)^{\frac{1}{2}}, \quad (15)$$

and  $\Gamma(\cdot)$  is the Gamma function.

*Proof.* Based on the definitions of Laplacian tensor and  $k$ -mode unfolding, the matrix  $\mathbf{L}_k \mathbf{L}_k^\top \in \mathbb{R}^{n \times n}$  is given by

$$\mathbf{L}_k \mathbf{L}_k^\top = \begin{bmatrix} d & \rho & \rho & \dots & \rho \\ \rho & d & \rho & \dots & \rho \\ \rho & \rho & d & \dots & \rho \\ \vdots & \vdots & \vdots & \ddots & \vdots \\ \rho & \rho & \rho & \dots & d \end{bmatrix},$$

where,

$$d = \binom{n-1}{k-1}^2 + \binom{n-1}{k-1} \frac{1}{(k-1)!}, \quad \text{and } \rho = \frac{T_{n-k}}{(k-1)!^2}.$$

Here  $\binom{n}{k} = \frac{n!}{(n-k)!k!}$  returns the binomial coefficients, and  $T_m$  are the  $k$ -simplex numbers (e.g., when  $k=3$ ,  $T_m$  are the triangular numbers). Moreover, the eigenvalues of  $\mathbf{L}_k \mathbf{L}_k^\top$  are  $d-\rho$  with multiplicity  $n-1$  and  $d+(n-1)\rho$  with multiplicity 1. Hence, the result is followed immediately. We write all the expressions using the Gamma function for simplicity.  $\square$

According to Proposition 1 and 2, every  $k$ -uniform hypergraph can achieve the minimum tensor entropy, while the maximum tensor entropy can be achieved only when the  $k$ -uniform hypergraph satisfies  $\text{mod}(n, k) = 0$  where  $\text{mod}$  refers to the MATLAB modulo operation. From Proposition 4, for arbitrary  $k$ -uniform hypergraph with  $n$  vertices and  $k \geq 3$ ,  $S_c$  could be smaller than the entropies of other  $d$ -regular hypergraphs for the same  $n$  and  $k$ . Nevertheless, in section 3, we will show evidence that the tensor entropy (10) is a measure of regularity for uniform hypergraphs. Large tensor entropy is characterized by the large number of connected vertices, high uniformity of vertex degrees, short path lengths, low clustering coefficients and high level of nontrivial symmetry, and the tensor entropy is small for hypergraphs with large cliques, long path lengths and high clustering coefficients, i.e., hypergraphs in which the vertices form highly connected clusters.

### 2.3 Numerical method via tensor trains

In reality, hypergraphs like co-authorship networks and protein-protein interaction networks exist in a very large scale, and computing the tensor entropy using the economy-size matrix SVD could be computationally expensive. Klus et al. [48] exploited TTD to efficiently calculate the Moore-Penrose (MP) inverse of the matrix obtained from any chosen unfolding of a given tensor. TTD provides a good compromise between numerical stability and level of compression, and has an associated algebra that facilitates computations. We thus adapt the framework of Klus et al. for the computation of the tensor entropy, see Algorithm 2. In step 2, we assume that the construction of adjacency and degree tensors in the TT-format can be achieved due to their simple structures. In step 4, the left- and right-orthonormalization

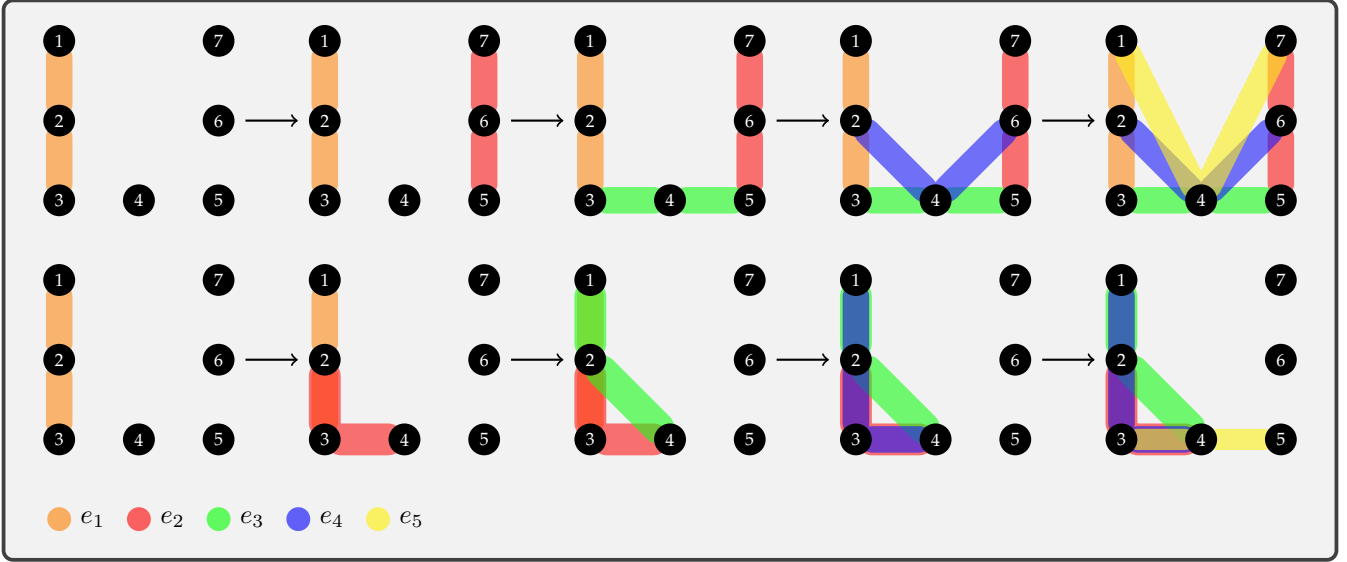


Figure 3. **Tensor entropy maximization/minimization.** The top row describes the first five stages of the tensor entropy maximization evolution with a growing number of hyperedges in the order of  $e_1 = \{1, 2, 3\}$ ,  $e_2 = \{5, 6, 7\}$ ,  $e_3 = \{3, 4, 5\}$ ,  $e_4 = \{2, 4, 6\}$  and  $e_5 = \{1, 4, 7\}$ . The bottom row reports the first five stages of the tensor entropy minimization process with a growing number of hyperedges in the order of  $e_1 = \{1, 2, 3\}$ ,  $e_2 = \{2, 3, 4\}$ ,  $e_3 = \{1, 2, 4\}$ ,  $e_4 = \{1, 3, 4\}$  and  $e_5 = \{3, 4, 5\}$ .

algorithms can be found in [48]. The computation and memory complexities of Algorithm 2 are estimated as  $\mathcal{O}(knr^3)$  and  $\mathcal{O}(knr^2)$ , respectively, where  $r$  can be viewed as the “average” rank of the TT-ranks. Clearly, both complexities are much lower than those from Algorithm 1 when  $r$  is small.

---

#### Algorithm 2: Computing tensor entropy from TTD

---

- 1: Given a  $k$ -uniform hypergraph  $\mathbf{G}$  with  $n$  vertices
  - 2: Construct the adjacency and degree tensors  $\mathbf{A}, \mathbf{D} \in \mathbb{R}^{n \times n \times \dots \times n}$  in the TT-format from  $\mathbf{G}$
  - 3: Compute the Laplacian tensor  $\mathbf{L} = \mathbf{D} - \mathbf{A}$  with core tensors  $\mathbf{X}^{(p)}$  and TT-ranks  $\{R_0, R_1, \dots, R_k\}$  based on the tensor train summation operation
  - 4: Left-orthonormalize the first  $k - 2$  cores and right-orthonormalize the last core of  $\mathbf{L}$
  - 5: Compute the economy-size matrix SVD of  $\bar{\mathbf{X}}^{(k-1)}$ , i.e.,  $\bar{\mathbf{X}}^{(k-1)} = \mathbf{USV}^\top$  for  $s = \text{rank}(\mathbf{S})$  and let  $\{\gamma_j\}_{j=1}^s = \text{diag}(\mathbf{S})$
  - 6: Set  $\hat{\gamma}_j = \frac{\gamma_j}{\sum_{i=1}^s \gamma_i}$  and compute  $\mathbf{S} = -\sum_{j=1}^s \hat{\gamma}_j \ln \hat{\gamma}_j$
  - 7: **return** The tensor entropy  $\mathbf{S}$  of  $\mathbf{G}$ .
- 

### 3 EXPERIMENTS

All the numerical examples presented were performed on a Linux machine with 8 GB RAM and a 2.4 GHz Intel Core i5 processor in MATLAB 2018b. The last example (section 3.6) also used MATLAB TT-Toolbox 2.2 by Oseledets et al. [49].

#### 3.1 Hyperedge growth model

We consider the case where the number of vertices is fixed and new hyperedges are iteratively added to the uniform

hypergraph. Figure 3 presents the hyperedge growth evolution of a 3-uniform hypergraph with 7 vertices, and it describes the tensor entropy maximization and minimization evolutions. In addition to plotting the two entropy trajectories, we also compute some statistics of the structural properties including average shortest path length, index of dispersion of the degree distribution and average clustering coefficient of the hypergraphs during the two evolutions, see Figure 4. If the two vertices are disconnected, we set the distance between them to be 4 for the purpose of visualization. The index of dispersion of the vertex degree distribution measures the ratio of its variance to its mean. We define the average clustering coefficient for uniform hypergraphs as follows:

$$C_j = \frac{|\{e_{ilk} : v_i, v_l, v_k \in \mathbf{N}_j, e_{ilk} \in \mathbf{E}\}|}{\binom{|\mathbf{N}_j|}{k}} \quad (16)$$

$$\Rightarrow C_{\text{avg}} = \frac{1}{n} \sum_{j=1}^n C_j,$$

where,  $\mathbf{N}_j$  is the set of vertices that are immediately connected to  $v_j$ . If  $|\mathbf{N}_j| < k$ , we set  $C_j = 0$ .

Let's denote the hypergraphs that achieve maximum (or minimum) tensor entropy at step  $j$  as  $\mathbf{G}_{\text{max}}^{(j)}$  (or  $\mathbf{G}_{\text{min}}^{(j)}$ ) for  $j = 1, 2, \dots, 35$ . Similar to maximizing graph entropy, the vertices of  $\mathbf{G}_{\text{max}}^{(j)}$  tend to have “almost equal” or equal degree which leads to a low index of dispersion, see Figure 4C. In particular,  $\mathbf{G}_{\text{max}}^{(j)}$  are the  $\frac{k}{n}j$ -regular hypergraphs for the early stages of the evolution, i.e.,  $j = 7, 14$ , but as the hypergraph becomes dense and complex, it is possible that  $\mathbf{G}_{\text{max}}^{(j)}$  will miss the regularity, i.e.,  $j = 21$ . Based on the top row of Figure 3, maximizing the tensor entropy will first connect all the vertices and then prefer to choose lower degree vertices with larger average geodesic distances, i.e., finding the geodesic distances between each pair in the triples and taking the mean. Similarly, the average geodesic

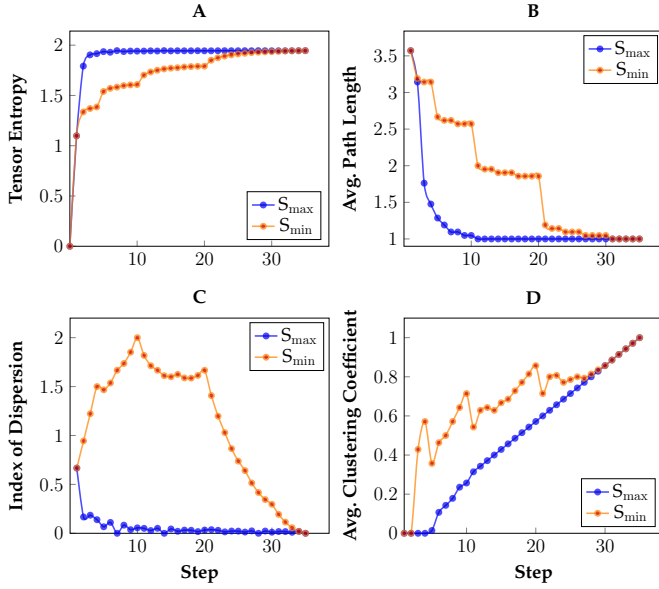


Figure 4. **Hyperedge growth model features.** (A), (B), (C) and (D) Trajectories of tensor entropy, average path length, index of dispersion and average clustering coefficient with respect to the hyperedge adding steps.

distances may lose importance if one wants to predict the next step as the hypergraph becomes complex. Furthermore, nontrivial symmetricity plays a role in maximizing the tensor entropy. For example, in  $G_{\max}^{(3)}$ , the vertices  $\{1, 2, 6\}$  and  $\{2, 4, 6\}$  have the same average geodesic distances (both are equal to  $\frac{7}{3}$ ), and the maximized tensor entropy returns the more symmetric  $G_{\max}^{(4)}$ . We also find that candidate hyperedges that intersect more existing hyperedges would return higher tensor entropy, which also explains the above example. However, there exists one huge disparity between the von Neumann graph entropy and the tensor entropy. The tensor entropy can temporarily decrease during the maximizing process as seen in Figure 4A. We observe that once the maximization evolution reaches some regularity or high level of nontrivial symmetricity, and the next step breaks such regularity or symmetricity, the tensor entropy will decrease. In other words, for these highly regular or highly symmetric  $G_{\max}^{(j)}$ , the corresponding tensor entropies  $S_{\max}^{(j)}$  achieve local maxima. This also explains why it is hard to determine the maximum of the tensor entropy for arbitrary uniform hypergraphs. On the other hand,  $S_{\min}^{(j)}$ , the tensor entropies of  $G_{\min}^{(j)}$  are similar to the von Neumann graph entropy. Minimizing the tensor entropy would result in the formations of complete sub-hypergraphs (*cliques*), see the bottom row of Figure 3. We can detect large jumps and drops in the next steps after completions of the sub-hypergraphs in Figure 4A and 4B, respectively. In order to make the discoveries more convincing, we repeated the same processes for  $k$ -uniform hypergraphs with different number of vertices and values of  $k$ , and observed similar results.

### 3.2 The Watts–Strogatz model

We perform an experiment on a synthetic random uniform hypergraph  $G$  with  $n = 100$  and  $k = 4$ . Similar to the Watts–

Strogatz graph, the initial hypergraph is 2-regular with lattice structure. Let  $q$  be the number of hyperedges added to the hypergraph in order to form *cliques* in every five vertices, and  $p$  be the rewiring probability of hyperedges, see Figure 5. Then  $G^{(q)}(p)$  denotes the random uniform hypergraphs generated by the rewiring probability  $p$  for different  $q$ . Particularly, when  $q = 3$ , the tensor entropy  $S^{(3)}(0) = 4.5527$ , the average clustering coefficient  $\alpha^{(3)}(0) = 0.7571$  and the average path length  $l^{(3)}(0) = 7.0606$ . The goal of the experiment is to explore the relations between the tensor entropy, the average clustering coefficient and path length with increasing the hyperedge rewiring probability  $p$  for different  $q$ . We also calculate the small world coefficient for each random hypergraph defined by

$$\sigma^{(q)}(p) = \frac{\alpha^{(q)}(p)/\alpha_{\text{rand}}^{(q)}}{l^{(q)}(p)/l_{\text{rand}}^{(q)}}, \quad (17)$$

where,  $\alpha_{\text{rand}}^{(q)}$  and  $l_{\text{rand}}^{(q)}$  are the average clustering coefficient and path length of its equivalent random uniform hypergraph, respectively [50]. For each  $G^{(q)}(p)$ , we compute its tensor entropy, average clustering coefficient, average path length and small world coefficient 10 times and take the means. We do not include the case of  $q = 1$  since it would likely result in non-connected random hypergraphs.

The results are shown in Figure 6. In general, with increasing rewiring probability  $p$ , the tensor entropy decays for both  $q = 2$  and  $3$ , see Figure 6A. When  $p < 0.1$ , the tensor entropies for  $q = 2$  are higher than these for  $q = 3$ . Based on the previous results, this may be because  $G^{(2)}(p)$  have lower average clustering coefficients with similar average path lengths compared to  $G^{(3)}(p)$ . When  $p > 0.1$ , the tensor entropies for  $q = 3$  is higher than these for  $q = 2$  likely due to  $G^{(3)}(p)$  having lower average path lengths with similar average clustering coefficients compared to  $G^{(2)}(p)$ . Moreover, the curves of the small world coefficient in Figure 6B are very similar to the one in the Watts–Strogatz graph, in which it grows gradually for  $p < 0.1$  and decreases quickly after  $p > 0.1$ . When the rewiring probability  $p$  is between 0.03 and 0.1,  $G^{(3)}(p)$  have apparent small world characteristics, e.g.,  $\alpha^{(3)}(0.07) = 0.5488$  and  $l^{(3)}(0.07) = 3.5748$ , over the 100 vertices. In addition, we find that the average clustering coefficient pattern is similar to tensor entropy. On the contrary, the average path length has a different trend. It decreases faster at small  $p$  and more slowly than the average clustering coefficient at large  $p$ , see Figure 6C. We also see a strictly positive correlation between the tensor entropy and the average clustering coefficient for  $q = 3$  in Figure 6D.

### 3.3 Primary school contact

The primary school contact dataset contains the temporal network of face-to-face contacts amongst the children and teachers (242 people in total) at a primary school, in which an active contact can include more than two people [51], [52]. In this study, we consider the cases of two-person contacts (i.e., a normal graph) and three-person contacts (i.e., a 3-uniform hypergraph) per hour, and observe how the contact frequencies change over one school day using tensor entropy. It can be used to quantify the respiratory

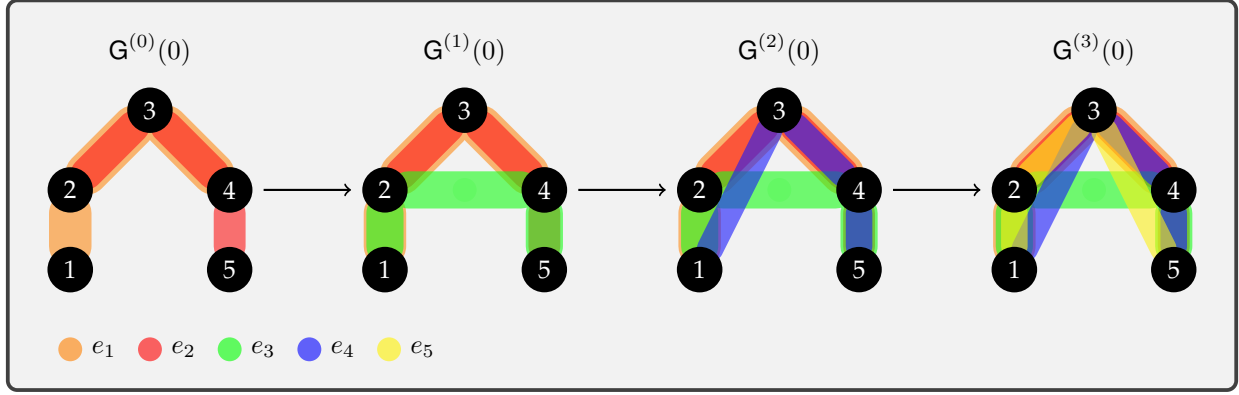


Figure 5. **Initial hypergraphs' structures for different  $q$ .** The plot describes the *cliques'* formation in the first five vertices of the uniform hypergraph with the rewiring probability zero, in which  $e_1 = \{1, 2, 3, 4\}$ ,  $e_2 = \{2, 3, 4, 5\}$ ,  $e_3 = \{1, 2, 4, 5\}$ ,  $e_4 = \{1, 3, 4, 5\}$  and  $e_5 = \{1, 2, 3, 5\}$ . The rest have the same patterns in every five vertices for a corresponding  $q$ .

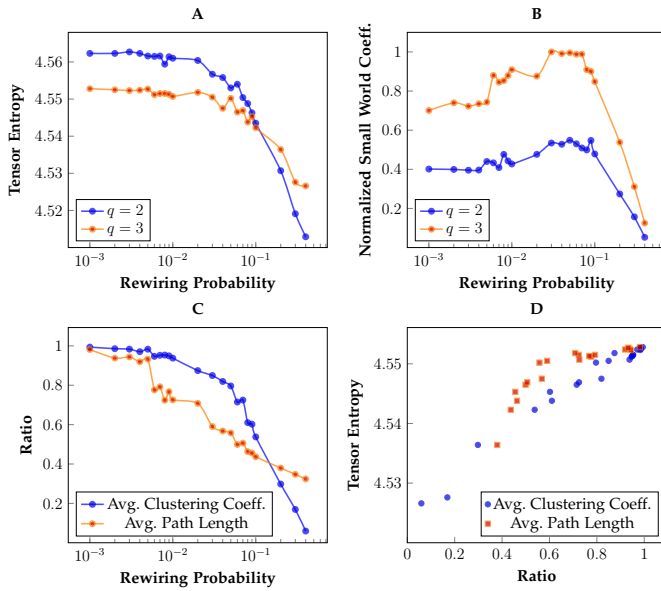


Figure 6. **The Watts–Strogatz model features.** (A) Tensor entropies of random uniform hypergraphs with different rewiring probabilities for different  $q$ . (B) Normalized small world coefficients of random uniform hypergraphs with different rewiring probabilities for different  $q$ . (C) Ratios  $\alpha^{(3)}(p)/\alpha^{(3)}(0)$  and  $l^{(3)}(p)/l^{(3)}(0)$  of random uniform hypergraphs with different rewiring probabilities for  $q = 3$ . (D) Scatter plot between the tensor entropy and the two ratios from (C).

infection transmission chances, and estimate transmission risks over multiple-person contacts. The results are shown in Figure 7, in which the two entropies have a similar and reasonable pattern. Both two-person and three-person contacts are more active at the second and eighth hours, and are less active at the fifth hour. Like the von Neumann entropy ( $k = 2$ ), the tensor entropy ( $k = 3$ ) is expected to grow with increased number of connected vertices, see Figure 7B and 7C, which implies that more children and teachers involved will yield larger tensor entropies. On the other hand, the entropy also heavily relies on the complexity and regularity of the uniform hypergraphs as demonstrated before. For instance, the number of people involved at the seventh hour is greater than that at the fifth hour for  $k = 3$ ,

but the tensor entropies are opposite because more contacts are made at the fifth hour, increasing the complexity or regularity in the uniform hypergraph, see Figure 7A.

### 3.4 Mouse neuron endomicroscopy

The goal of the experiment is to observe mouse neuron activation patterns using fluorescence across space and time before and after food treatment in the mouse hypothalamus. Large changes in fluorescence are inferred to be active neurons that are “firing.” The mouse endomicroscopy dataset is an imaging video created under the 10-minute periods of feeding, fasting and re-feeding. The imaging region contains in total 20 neuron cells, and the levels of “firing” are also recorded for each neuron. In this study, we build  $k$ -uniform hypergraphs for each 10-minute interval based on the correlations/multi-correlations of the neuron “firing” level for  $k = 2, 3$ . The multi-correlation among three variables is defined by

$$r^2 = c_1^2 + c_2^2 + c_3^2 - 2c_1c_2c_3, \quad (18)$$

where,  $c_1$ ,  $c_2$  and  $c_3$  are the correlations between the three variables [53]. It turns out that the multi-correlation is a generalization of Pearson correlation which can measure the strength of multivariate correlation. The results are shown in Figure 8, in which (A), (B) and (C) are the first eigenfaces of the corresponding three phases showing the dominant features in these phases. For computing the entropy, we choose the cutoff threshold to be 0.93 in the construction of edge/hyperedge. In Figure 8D, the von Neumann entropy ( $k = 2$ ) stays constant, while the tensor entropy ( $k = 3$ ) is able to exhibit the neuron activity level changes, in which it is lower during the fast phase and higher during the fed/re-fed phase. If we lower the threshold, a similar pattern can also be observed for  $k = 2$ . More interestingly, we find that the two hypergraphs for the fed and re-fed phases contain a number of common hyperedges, and these hyperedges are mainly composed of vertices with high degrees. It implies that these neurons may be involved in the eating process for mice. Such phenomena is barely seen in the corresponding graphs for high thresholds. Therefore, the mouse neuron activation patterns can be more accurately captured through

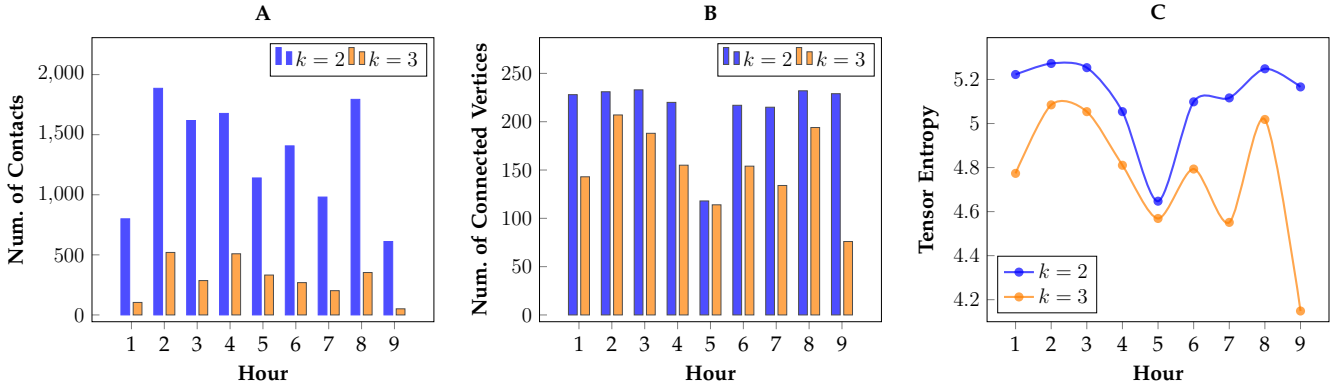


Figure 7. **Primary school contact features.** (A) Number of the two-person and three-person contacts amongst the children and teachers every one hour of a day. (B) Number of children and teachers involved every one hour of a day in the two-person and three-person contacts, respectively. (C) Trajectories of the von Neumann entropy and the tensor entropy for the two-person and three-person contacts of a day.

3-uniform hypergraphs, i.e., more than two neurons “co-fire” or work together in the mouse hypothalamus.

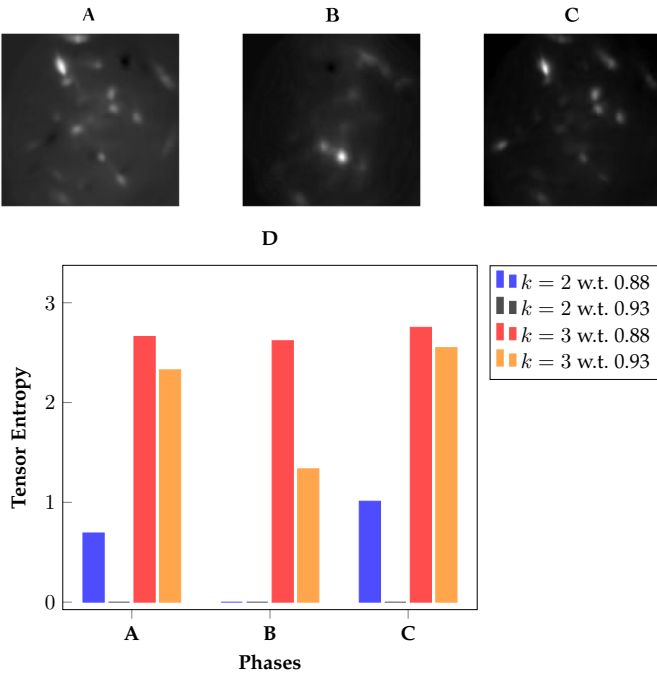


Figure 8. **Mouse neuron endomicroscopy features.** (A), (B) and (C) First eigenfaces of the three phases - fed, fast and re-fed. (D) Tensor entropies of the  $k$ -uniform hypergraphs constructed from the corresponding three phases with  $k = 2, 3$  (here w.t. stands for “with threshold”).

### 3.5 Cellular reprogramming

Cellular reprogramming is a process that introduces specialized proteins called transcription factors as a control mechanism to transform one cell type to another. Unbiased technologies such as genome-wide chromosome conformation capture (Hi-C) are applied to capture the dynamics of reprogramming [5], [6], [55]. However, the pairwise contacts from Hi-C data fail to include the multiway interactions of chromatin. Furthermore, the notion of transcription factories supports the existence of simultaneous interactions involving multiple genomic loci [54], implying that

the human genome configuration can be represented by a hypergraph. Therefore, in this example, we use 3-uniform hypergraphs to partially recover the 3D configuration of the genome based on the multi-correlation (18) from Hi-C matrices. We believe that such reconstruction can provide more information about the genome structure and patterns, compared to the pairwise Hi-C contacts. We use a cellular reprogramming dataset, containing normalized Hi-C data from fibroblast proliferation and MyoD-mediated fibroblast reprogramming (MyoD is the transcription factor used for control) for Chromosome 14 at 1MB resolution with a total of 89 genomic loci. Our goal is to quantitatively detect a bifurcation between the fibroblast proliferation and reprogramming data, and accurately identify the critical transition point between cell identities during reprogramming. The results are shown in Figure 9. We can clearly observe a bifurcation between the two trajectories using the tensor entropy of the 3-uniform hypergraphs recovered from the Hi-C measurements. Crucially, the critical transition point marked in Figure 9A is consistent with the ground-truth statistic provided in [55]. In contrast, the von Neumann entropy cannot provide adequate information about the bifurcation and critical transition point, if one analyzes the Hi-C measurements as adjacency matrices. The two trajectories are separate from the beginning, see Figure 9B.

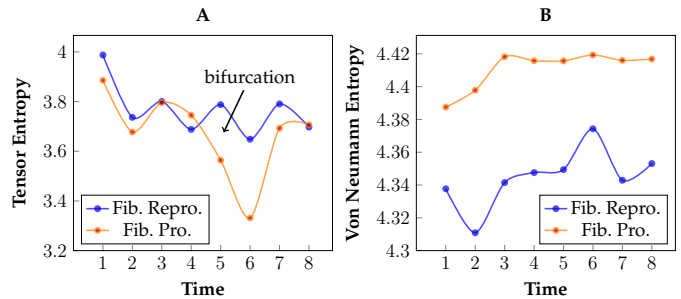


Figure 9. **Cellular reprogramming features.** (A) Tensor entropies of the uniform hypergraphs recovered from Hi-C measurements with multi-correlation cutoff threshold 0.95. (B) Von Neuman entropies of the binarized Hi-C matrices with weight cutoff threshold 0.95.

### 3.6 Algorithm run time comparison

In this example, the  $k$ -uniform hypergraphs are constructed with  $n$  vertices by forming a strip structure in which every pair of connected hyperedges only contains one common vertex. We compare the computational efficiency of the SVD-based Algorithm 1 and the TTD-based Algorithm 2 in computing the tensor entropy. The results are shown in Figure 10. For the TTD-based entropy computations, we assume that all the adjacency and degree tensors of the uniform hypergraphs are already provided in the TT-format. Evidently, Algorithm 2 is more time efficient than Algorithm 1 for 4-uniform and 5-uniform hypergraphs with the strip structure as  $n$  becomes larger, see Figure 10. Particularly, when  $k = 5$ , the TTD-based algorithm exhibits a huge time advantage as predicted in the computation complexity. The time curve from the SVD-based Algorithm 1 increases exponentially, while it grows at a much slower rate if using Algorithm 2. In the meantime, we compute the relative errors between the tensor entropies computed from the two algorithms, all of which are within  $10^{-15}$ .

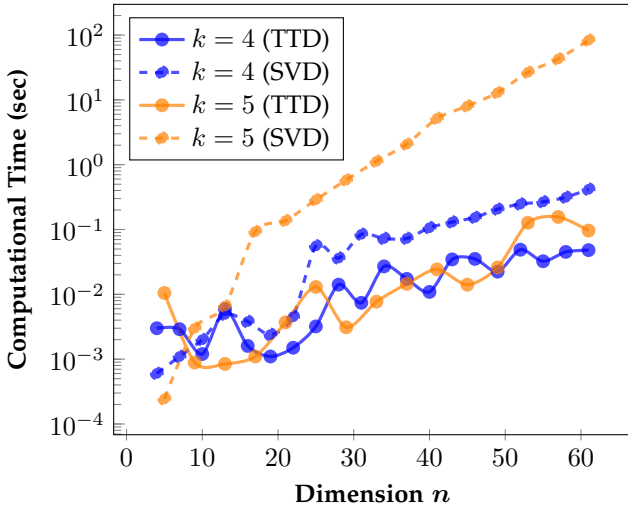


Figure 10. **Computational time comparisons between the SVD-based and TTD-based algorithms.** For the TTD-based entropy computations, we report the times of left- and right-orthonormalization and economy-size matrix SVD. For the SVD-based entropy computations, we only report the time of economy-size matrix SVD.

## 4 DISCUSSION

The first five numerical examples reported here highlight that the  $k$ -mode singular values computed from the HOSVD of the Laplacian tensors can provide nice predictions of structural properties for uniform hypergraphs. This method can also be used for anomaly detection in the context of dynamics as we demonstrated in the mouse neuron endomicroscopy and cellular reprogramming datasets. However, more theoretical and numerical investigations are required to assess the real advantages of hypergraphs versus normal graphs, and is an important avenue of future research. Moreover, as we pointed out in section 2.3, many simple structure tensors can be directly created in the TT-format without requiring construction of the full representations. For example, Oseledets et al. [49] built the Laplacian operator in the TT-format for the discretized heat equations.

We believe that similar results can happen to the adjacency, degree and Laplacian tensors for uniform hypergraphs.

Instead of looking at the  $k$ -mode singular values, we can consider the tensor eigenvalues in defining the tensor entropy. We will refer to it as the eigenvalue entropy later. See Appendix A for a short introduction to tensor eigenvalues for supersymmetric tensors. Based on the tensor eigenvalue formulations, we can establish the eigenvalue entropy measure for uniform hypergraphs.

**Definition 2.** Let  $\mathbf{G}$  be a  $k$ -uniform hypergraph with  $n$  vertices. The eigenvalue entropy of  $\mathbf{G}$  is defined by

$$S = - \sum_{j=1}^d |\hat{\lambda}_j| \ln |\hat{\lambda}_j|, \quad (19)$$

where,  $|\hat{\lambda}_j|$  are the normalized modulus of the eigenvalues of the Laplacian tensor  $\mathbf{L}$  such that  $\sum_{j=1}^d |\hat{\lambda}_j| = 1$ , and  $d = n(k-1)^{n-1}$  is the total number of the eigenvalues.

The convention  $0 \ln 0 = 0$  is used if  $|\hat{\lambda}_j| = 0$ . We can use other tensor eigenvalue notions including H-eigenvalue, E-eigenvalue and Z-eigenvalue with a corresponding  $d$  to fit into the formula. For curiosity, we repeat the hyperedge growth model using the eigenvalue entropy, see Figure 11. The entropy minimization evolution trajectory is the same for the first five stages in which cliques are formed. The maximization evolution trajectory becomes different from the fourth stage after the hypergraph is connected, in which short path lengths and high level of nontrivial symmetricity are no longer the factors that maximize the entropy. In addition, computing the eigenvalues of a tensor is an NP hard problem [56]. The tensor eigenvalue solvers in the MATLAB Toolbox TenEig [57], [58] become computationally expensive and inaccurate when the size of Laplacian tensors is large. Hence, the eigenvalue entropy may not be used to predict the structural properties for uniform hypergraphs, but it might contain other unknown features that are required to explore in the future. Similarly for the H-eigenvalue, E-eigenvalue and Z-eigenvalue entropy measures.

Furthermore, the notion of robustness for uniform hypergraphs is an important topic. In graph theory, one of the popular measures is called effective resistance [59]. The authors in [60] show that the effective graph resistance can be written in terms of the reciprocals of graph Laplacian eigenvalues, and robust networks have small effective graph resistance. Hence, we attempt to establish similar relationship using the  $k$ -mode singular values from the Laplacian tensors to describe the robustness of uniform hypergraphs.

**Definition 3.** Let  $\mathbf{G}$  be a connected  $k$ -uniform hypergraph with  $n$  vertices. The effective resistance of  $\mathbf{G}$  is defined by

$$R = n \sum_{j=1}^n \frac{1}{\gamma_j}, \quad (20)$$

where,  $\gamma_j$  are the  $k$ -mode singular values of  $\mathbf{L}$ .

If a uniform hypergraph is non-connected, then the effective resistance  $R = \infty$ . Based on (20), we compute the effective resistance of the uniform hypergraphs  $\mathbf{G}_{\max}^{(j)}$  in the hyperedge growth model example, denoted by  $R_{\max}^{(j)}$ . Similar to the effective graph resistance,  $R_{\max}^{(j)}$  strictly decreases

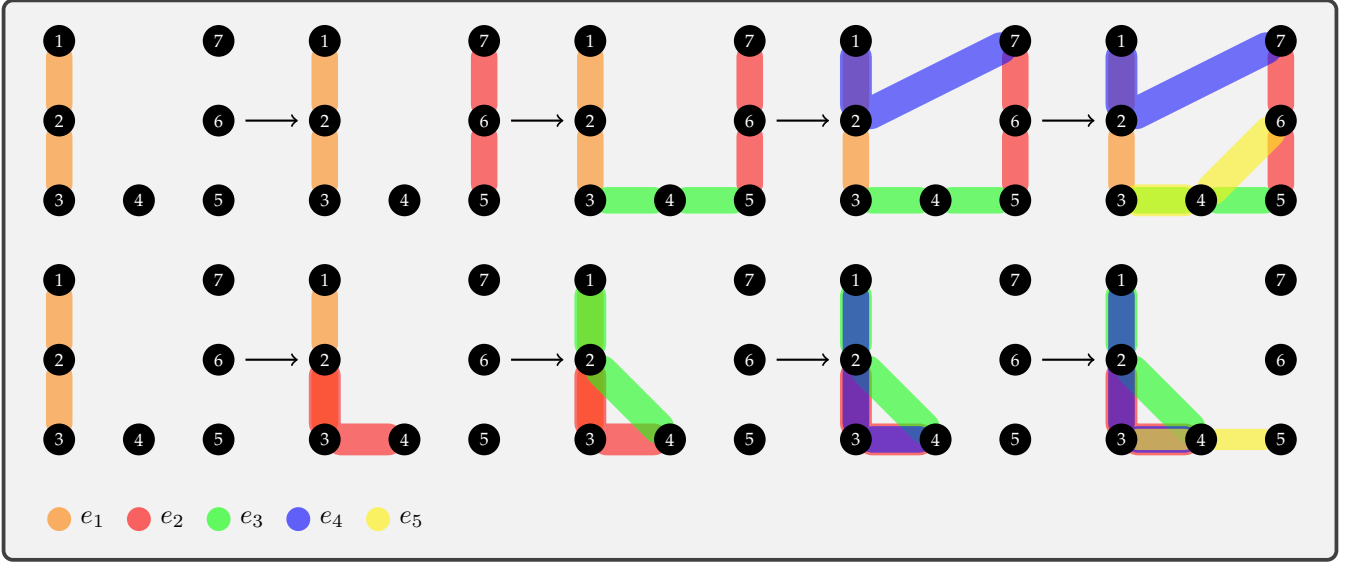


Figure 11. **Eigenvalue entropy maximization/minimization.** The top row describes the first five stages of the eigenvalue entropy maximization evolution with a growing number of hyperedges in the order of  $e_1 = \{1, 2, 3\}$ ,  $e_2 = \{5, 6, 7\}$ ,  $e_3 = \{3, 4, 5\}$ ,  $e_4 = \{1, 2, 7\}$  and  $e_5 = \{3, 4, 6\}$ . The eigenvalue entropy  $S_{\max}^{(j)} = 4.4910, 5.6342, 5.8608, 5.9490$  and  $6.0091$  for  $j = 1, 2, 3, 4, 5$ . The bottom row reports the first five stages of the eigenvalue entropy minimization process with a growing number of hyperedges in the order of  $e_1 = \{1, 2, 3\}$ ,  $e_2 = \{2, 3, 4\}$ ,  $e_3 = \{1, 2, 4\}$ ,  $e_4 = \{1, 3, 4\}$  and  $e_5 = \{3, 4, 5\}$ . The eigenvalue entropy  $S_{\min}^{(j)} = 4.4910, 5.3604, 5.4434, 5.4715$  and  $5.6334$  for  $j = 1, 2, 3, 4, 5$ . All the tensor eigenvalues of the Laplacian tensors in this experiment are computed from the MATLAB Toolbox TenEig.

when hyperedges are added and achieves the minimum at the final step when the hypergraph is complete, see Table 1. We can also expect that the smaller the effective resistance is, the more robust the uniform hypergraph. We believe that the effective resistance (20) is a good measure for uniform hypergraph robustness, but more theoretical and numerical support is needed to verify this hypothesis.

Table 1  
The effective resistance and tensor entropy.

Step	$j = 3$	$j = 5$	$j = 15$	$j = 25$	$j = 35$
$R_{\max}^{(j)}$	34.8384	20.9432	7.3863	4.4819	3.2166
$S_{\max}^{(j)}$	1.9037	1.9359	1.9430	1.9448	1.9456

## 5 CONCLUSION

In this paper, we proposed a new notion of entropy for uniform hypergraphs based on the tensor higher-order singular value decomposition. The  $k$ -mode singular values of Laplacian tensors provide nice interpretations regarding the structural properties of uniform hypergraphs. The tensor entropy heavily depends on the vertex degrees, path lengths, clustering coefficients and nontrivial symmetry. We investigated the lower and upper bounds of the entropy and provided the entropy formula for complete uniform hypergraphs. A TTD-based computational framework is proposed for computing the tensor entropy efficiently. We also applied this spectral measure to real biological networks for anomaly detection, and achieve better performances compared to the von Neumann graph entropy. As discussed in section 4, the detailed relations between tensor eigenvalues and entropy, and the theoretical investigations of hypergraph robustness require further exploration. Controllability and

influenceability of uniform hypergraphs are also important for future research.

## APPENDIX A TENSOR EIGENVALUES

The tensor eigenvalue problems of real supersymmetric tensors were first explored by Qi [61], [62] and Lim [63] independently. There are different notions of tensor eigenvalue, in which the most frequent used are eigenvalues and E-eigenvalues. The eigenvalues  $\lambda \in \mathbb{R}$  and eigenvectors  $\mathbf{v} \in \mathbb{R}^n$  of a  $k$ -th order supersymmetric tensor  $\mathbf{X} \in \mathbb{R}^{n \times n \times \dots \times n}$  are defined as follows:

$$\mathbf{X} \times \mathbf{v}^{k-1} = \lambda \mathbf{v}^{[k-1]}, \quad (21)$$

where,  $\mathbf{X} \times \mathbf{v}^{k-1} = \mathbf{X} \times_1 \mathbf{v} \times_2 \dots \times_{k-1} \mathbf{v}$  and  $\mathbf{v}^{[k-1]}$  stands for the element-wise  $(k-1)$ -th power of  $\mathbf{v}$ . The eigenvalues  $\lambda$  could be complex, and if  $\lambda$  are real, we call them H-eigenvalues. The behaviors of tensor eigenvalues are close to eigenvalues of matrices. There is a total of  $n(k-1)^{n-1}$  eigenpairs. The sum of all eigenvalues are equal to  $(k-1)^{n-1} \text{trace}(\mathbf{X})$  where  $\text{trace}(\mathbf{X}) = \sum_{j=1}^n X_{j,j,\dots,j}$ , and the product of all eigenvalues are equal to the hyperdeterminant  $\det(\mathbf{X})$ , the resultant of  $\mathbf{X} \times \mathbf{v}^{k-1} = \mathbf{0}$ .

Second, the E-eigenvalues  $\lambda \in \mathbb{R}$  and E-eigenvectors  $\mathbf{v} \in \mathbb{R}^n$  of a  $k$ -th order supersymmetric tensor  $\mathbf{X} \in \mathbb{R}^{n \times n \times \dots \times n}$  are defined as follows:

$$\begin{cases} \mathbf{X} \times \mathbf{v}^{k-1} = \lambda \mathbf{v} \\ \mathbf{v}^T \mathbf{v} = 1 \end{cases} \quad (22)$$

The E-eigenvalues  $\lambda$  could be complex, and if  $\lambda$  are real, we call them Z-eigenvalues. Although the spectral properties of E-eigenvalues are still not fully understood, Chen et al. [64] showed that the Z-eigenvector associated with the second

smallest Z-eigenvalue of a normalized Laplacian tensor can be used for hypergraph partition.

## ACKNOWLEDGMENT

We thank Dr. Frederick Leve at the Air Force Office of Scientific Research (AFOSR) for support and encouragement. This work is supported in part under AFOSR Award No: FA9550-18-1-0028, Smale Institute, and the Lifelong Learning Machines program from DARPA/MTO.

## REFERENCES

- [1] L. A. N. Amaral, A. Scala, M. Barthélemy, and H. E. Stanley, "Classes of small-world networks," *Proceedings of the National Academy of Sciences*, vol. 97, no. 21, pp. 11 149–11 152, 2000. [Online]. Available: <https://www.pnas.org/content/97/21/11149>
- [2] A. Barabasi and E. Bonabeau, "Scale-free networks," *Scientific American*, vol. 288, 2003. [Online]. Available: <http://dx.doi.org/10.1038/scientificamerican0503-60>
- [3] J. Kleinberg, "Navigation in a small world," *Nature*, vol. 406, 2000.
- [4] D. Watts and S. Strogatz, "Collective dynamics of "small-world" networks," *Nature*, vol. 393, 1998.
- [5] I. Rajapakse and M. Groudine, "On emerging nuclear order," *The Journal of Cell Biology*, vol. 192, no. 5, pp. 711–721, 2011. [Online]. Available: <http://jcb.rupress.org/content/192/5/711>
- [6] T. Ried and I. Rajapakse, "The 4d nucleome," *Methods*, vol. 123, pp. 1–2, 2017, the 4D Nucleome. [Online]. Available: <http://www.sciencedirect.com/science/article/pii/S1046202317302220>
- [7] M. Karsai, N. Perra, and A. Vespignani, "Time varying networks and the weakness of strong ties," *Sci Rep*, vol. 4, 2015.
- [8] N. D. Monnig and F. G. Meyer, "The resistance perturbation distance: A metric for the analysis of dynamic networks," *Discrete Applied Mathematics*, vol. 236, pp. 347–386, 2018. [Online]. Available: <http://www.sciencedirect.com/science/article/pii/S0166218X17304626>
- [9] S. Ranshous, S. Shen, D. Koutra, S. Harenberg, C. Faloutsos, and N. F. Samatova, "Anomaly detection in dynamic networks: A survey," *WIREs Comput. Stat.*, vol. 7, no. 3, pp. 223–247, May 2015. [Online]. Available: <https://doi.org/10.1002/wics.1347>
- [10] L. Akoglu, H. Tong, and D. Koutra, "Graph based anomaly detection and description: A survey," *Data Mining and Knowledge Discovery*, vol. 29, no. 3, pp. 626–688, 4 2015.
- [11] D. A. Papadimitriou, P. and Garcia-Molina, "Mitigation of infectious disease at school: targeted class closure vs school closure," *J Internet Serv Appl*, vol. 1, pp. 19–30, 2010.
- [12] S.-H. Cha, "Comprehensive survey on distance/similarity measures between probability density functions," *International Journal of Mathematical Models and Methods in Applied Sciences*, vol. 1, no. 4, pp. 300–307, 2007. [Online]. Available: <http://www.gly.fsu.edu/~parker/geostats/Cha.pdf>
- [13] R. W. Hamming, "Error detecting and error correcting codes," *The Bell System Technical Journal*, vol. 29, no. 2, pp. 147–160, April 1950.
- [14] W. D. LEVANDOWSKY, M., "Distance between sets," *Nature*, vol. 234, pp. 34–35, 1971.
- [15] C. Donnat and S. Holmes, "Tracking network dynamics: A survey using graph distances," *The annals of applied statistics*, vol. 12, p. 971, 2018.
- [16] G. Simonyi, "Graph entropy: A survey," in *Combinatorial Optimization*, 1993.
- [17] C. Donnat and S. Holmes, "Discovering important nodes through graph entropy the case of enron email database," in *LinkKDD '05: Proceedings of the 3rd international workshop on Link discovery*, 2005, pp. 74–81.
- [18] A. Li and Y. Pan, "Structural information and dynamical complexity of networks," *IEEE Transactions on Information Theory*, vol. 62, no. 6, pp. 3290–3339, June 2016.
- [19] S. Braunstein, S. Ghosh, T. Mansour, S. Severini, and R. C. Wilson, "Some families of density matrices for which separability is easily tested," *Physical Review A*, vol. 73, 2006.
- [20] G. Minello, L. Rossi, and A. Torsello, "On the von Neumann entropy of graphs," *Journal of Complex Networks*, vol. 7, no. 4, pp. 491–514, 11 2018. [Online]. Available: <https://doi.org/10.1093/comnet/cny028>
- [21] F. Passerini and S. Severini, "The von neumann entropy of networks," 2008. [Online]. Available: <https://arxiv.org/abs/0812.2597>
- [22] M. M. Wolf, A. M. Klinvex, and D. M. Dunlavy, "Advantages to modeling relational data using hypergraphs versus graphs," in *2016 IEEE High Performance Extreme Computing Conference (HPEC)*, Sep. 2016, pp. 1–7.
- [23] C. Berge, *Hypergraphs, Combinatorics of Finite Sets, Third Edition*. North-Holland, Amsterdam, 1989.
- [24] M. Newman, *Networks: An Introduction*. OUP Oxford, 2010. [Online]. Available: <https://books.google.com/books?id=q7HVtpYVfC0C>
- [25] C. Chen, A. Surana, A. Bloch, and I. Rajapakse, "Data-driven model reduction for multilinear control systems via tensor trains," *submitted*. [Online]. Available: <https://arxiv.org/abs/1912.03569>
- [26] A. Cichocki, N. Lee, I. Oseledets, A. Phan, Q. Zhao, and D. P. Mandic, *Tensor Networks for Dimensionality Reduction and Large-scale Optimization: Part 2 Applications and Future Perspectives*. now, 2017. [Online]. Available: <https://ieeexplore.ieee.org/document/8187112>
- [27] H. Lu, K. N. Plataniotis, and A. N. Venetsanopoulos, "MPCA: Multilinear principal component analysis of tensor objects," *IEEE Transactions on Neural Networks*, vol. 19, no. 1, pp. 18–39, Jan 2008.
- [28] W. Wang, V. Aggarwal, and S. Aeron, "Principal component analysis with tensor train subspace," *Pattern Recognition Letters*, vol. 122, pp. 86–91, 2019.
- [29] A. H. Williams, T. H. Kim, F. Wang, S. Vyas, S. I. Ryu, K. V. Shenoy, M. Schnitzer, T. G. Kolda, and S. Ganguli, "Unsupervised discovery of demixed, low-dimensional neural dynamics across multiple timescales through tensor component analysis," *Neuron*, vol. 98, no. 6, pp. 1099–1115.e8, 2018.
- [30] D. Hu, X. L. Li, X. G. Liu, and S. G. Zhang, "Extremality of graph entropy based on degrees of uniform hypergraphs with few edges," *Acta Mathematica Sinica, English Series*, vol. 35, no. 7, pp. 1238–1250, Jul 2019. [Online]. Available: <https://doi.org/10.1007/s10114-019-8093-2>
- [31] H. Wang, G. Xiao, Y. Yan, and D. Suter, "Searching for representative modes on hypergraphs for robust geometric model fitting," *IEEE Transactions on Pattern Analysis and Machine Intelligence*, vol. 41, no. 3, pp. 697–711, March 2019.
- [32] I. Bloch and A. Bretto, "A new entropy for hypergraphs," in *Discrete Geometry for Computer Imagery*, M. Couprie, J. Cousty, Y. Kenmochi, and N. Mustafa, Eds. Cham: Springer International Publishing, 2019, pp. 143–154.
- [33] L. De Lathauwer, B. De Moor, and J. Vandewalle, "A multilinear singular value decomposition," *SIAM Journal on Matrix Analysis and Applications*, vol. 21, no. 4, pp. 1253–1278, 2000.
- [34] T. G. Kolda and B. Bader, "Tensor decompositions and applications," *SIAM Review*, vol. 51, no. 3, pp. 455–500, 2009. [Online]. Available: <https://doi.org/10.1137/07070111X>
- [35] T. G. Kolda, "Multilinear operators for higher-order decompositions," 2006.
- [36] S. Ragnarsson and C. Van Loan, "Block tensor unfoldings," *SIAM J. Matrix Analysis Applications*, vol. 33, pp. 149–169, 2012.
- [37] C. Chen, A. Surana, A. Bloch, and I. Rajapakse, "Multilinear time invariant system theory," in *2019 Proceedings of the Conference on Control and its Applications*, pages 118–125, 2019. [Online]. Available: <https://epubs.siam.org/doi/abs/10.1137/1.9781611975758.18>
- [38] G. Bergqvist and E. G. Larsson, "The higher-order singular value decomposition: Theory and an application [lecture notes]," *IEEE Signal Processing Magazine*, vol. 27, no. 3, pp. 151–154, May 2010.
- [39] I. Oseledets, "Tensor-train decomposition," *SIAM Journal on Scientific Computing*, vol. 33, no. 5, pp. 2295–2317, 2011. [Online]. Available: <https://doi.org/10.1137/090752286>
- [40] A. Banerjee, A. Char, and B. Mondal, "Spectra of general hypergraphs," *Linear Algebra and its Applications*, vol. 518, pp. 14–30, 2017. [Online]. Available: <http://www.sciencedirect.com/science/article/pii/S0024379516306115>
- [41] J. Cooper and A. Dutle, "Spectra of uniform hypergraphs," *Linear Algebra and its Applications*, vol. 436, no. 9, pp. 3268–3292, 2012. [Online]. Available: <http://www.sciencedirect.com/science/article/pii/S0024379511007610>
- [42] S. Hu and L. Qi, "The eigenvectors associated with the zero eigenvalues of the laplacian and signless laplacian tensors of a uniform hypergraph," *Discrete Applied Mathematics*, vol. 169, pp. 140–151, 2014. [Online]. Available: <http://www.sciencedirect.com/science/article/pii/S0166218X14000031>

- [43] L. Qi, "H<sup>+</sup>-eigenvalues of laplacian and signless laplacian tensors," *Communications in Mathematical Sciences*, vol. 12, 03 2013.
- [44] S. Hu and L. Qi, "The laplacian of a uniform hypergraph," *Journal of Combinatorial Optimization*, vol. 29, no. 2, pp. 331–366, Feb 2015. [Online]. Available: <https://doi.org/10.1007/s10878-013-9596-x>
- [45] S. Hu, L. Qi, and J. Xie, "The largest laplacian and signless laplacian h-eigenvalues of a uniform hypergraph," *Linear Algebra and its Applications*, vol. 469, pp. 1–27, 2015. [Online]. Available: <http://www.sciencedirect.com/science/article/pii/S002437951400754X>
- [46] J. Xie and A. Chang, "On the z-eigenvalues of the adjacency tensors for uniform hypergraphs," *Linear Algebra and its Applications*, vol. 439, no. 8, pp. 2195–2204, 2013. [Online]. Available: <http://www.sciencedirect.com/science/article/pii/S0024379513004679>
- [47] S. Braunstein, S. Ghosh, and S. Severini, "The laplacian of a graph as a density matrix: A basic combinatorial approach to separability of mixed states," *Annals of Combinatorics*, vol. 10, 07 2004.
- [48] S. Klus, P. Gellß, S. Peitz, and C. Schütte, "Tensor-based dynamic mode decomposition," *Nonlinearity*, vol. 31, no. 7, pp. 3359–3380, Jun 2018. [Online]. Available: <https://doi.org/10.1088/2F1361-6544%2Faabc8f>
- [49] I. Oseledets, S. Dolgov, V. Kazeev, O. Lebedeva, and T. Mach, "Tt-toolbox," 2014, version 2.2.2. [Online]. Available: <https://github.com/oseledets/TT-Toolbox>
- [50] M. D. Humphries and K. Gurney, "Network 'small-world-ness': A quantitative method for determining canonical network equivalence," *PLOS ONE*, vol. 3, no. 4, pp. 1–10, 04 2008. [Online]. Available: <https://doi.org/10.1371/journal.pone.0002051>
- [51] B. A. Gemmetto, V. and C. Cattuto, "Mitigation of infectious disease at school: targeted class closure vs school closure," *BMC Infect Dis*, vol. 14, p. 695, 2014.
- [52] J. Stehla, N. Voirin, A. Barrat, C. Cattuto, L. Isella, J.-F. Pinton, M. Quaggiotto, W. Van den Broeck, C. Ragis, B. Lina, and P. Vanhems, "High-resolution measurements of face-to-face contact patterns in a primary school," *PLOS ONE*, vol. 6, no. 8, pp. 1–13, 08 2011. [Online]. Available: <https://doi.org/10.1371/journal.pone.0023176>
- [53] N. Zheng and Jianji Wang, "Measures of correlation for multiple variables," 2019. [Online]. Available: <https://arxiv.org/abs/1401.4827>
- [54] P. R. Cook and D. Marenduzzo, "Transcription-driven genome organization: a model for chromosome structure and the regulation of gene expression tested through simulations," *Nucleic Acids Research* vol. 46, no. 19, pp. 9895–9906, 2018. [Online]. Available: <https://academic.oup.com/nar/article/46/19/9895/5099447>
- [55] S. Liu, H. Chen, S. Ronquist, et al. "Genome architecture mediates transcriptional control of human myogenic reprogramming," *iScience* vol. 6, pp. 232–246, 2018a. [Online]. Available: <https://www.sciencedirect.com/science/article/pii/S2589004218301147>
- [56] C. J. Hillar and L.-H. Lim, "Most tensor problems are np-hard," *J. ACM*, vol. 60, no. 6, pp. 45:1–45:39, Nov. 2013. [Online]. Available: <http://doi.acm.org/10.1145/2512329>
- [57] L. Chen, L. Han, T.-Y. Li, and L. Zhou, "Teneig," 2015, version 2.0. [Online]. Available: <https://users.math.msu.edu/users/chenlipi/TenEig.html>
- [58] L. Chen, L. Han, and L. Zhou, "Computing tensor eigenvalues via homotopy methods," *SIAM Journal on Matrix Analysis and Applications*, vol. 37, no. 1, pp. 290–319, 2016. [Online]. Available: <https://doi.org/10.1137/15M1010725>
- [59] W. Ellens, F. Spieksma, P. V. Mieghem, A. Jamakovic, and R. Kooij, "Effective graph resistance," *Linear Algebra and its Applications*, vol. 435, no. 10, pp. 2491–2506, 2011, special Issue in Honor of Dragos Cvetkovic. [Online]. Available: <http://www.sciencedirect.com/science/article/pii/S0024379511001443>
- [60] D. Klein and M. Randic, "Resistance distance," *Journal of Mathematical Chemistry*, vol. 12, pp. 81–95, 1993.
- [61] L. Qi, "Eigenvalues of a real supersymmetric tensor," *Journal of Symbolic Computation*, vol. 40, no. 6, pp. 1302–1324, 2005. [Online]. Available: <http://www.sciencedirect.com/science/article/pii/S0747717105000817>
- [62] —, "Eigenvalues and invariants of tensors," *Journal of Mathematical Analysis and Applications*, vol. 325, no. 2, pp. 1363–1377, 2007. [Online]. Available: <http://www.sciencedirect.com/science/article/pii/S0022247X06001764>
- [63] L.-H. Lim, "Singular values and eigenvalues of tensors: A variational approach," vol. 2005, 01 2006, pp. 129–132.
- [64] Y. Chen, L. Qi, and X. Zhang, "The fiedler vector of a laplacian tensor for hypergraph partitioning," *SIAM Journal on Scientific Computing*, vol. 39, no. 6, pp. A2508–A2537, 2017. [Online]. Available: <https://doi.org/10.1137/16M1094828>